Mononuclear Polypyridylruthenium(II) Complexes with High Membrane Permeability in Gram-Negative Bacteria – In particular Pseudomonas aeruginosa

ARTICLE *in* CHEMISTRY - A EUROPEAN JOURNAL · JUNE 2015

Impact Factor: 5.73 · DOI: 10.1002/chem.201500385

7 AUTHORS, INCLUDING:

Anil Gorle

Griffith University

4 PUBLICATIONS **10** CITATIONS

SEE PROFILE

Marshall Feterl

James Cook University

10 PUBLICATIONS **131** CITATIONS

SEE PROFILE

Jeffrey Warner

James Cook University

45 PUBLICATIONS **471** CITATIONS

SEE PROFILE

Constantin C Constantinoiu

James Cook University

31 PUBLICATIONS **119** CITATIONS

SEE PROFILE

ChemPubSoc Europe

DOI: 10.1002/chem.201500385

CHEMISTRY
A European Journal
Full Paper

Metal-Based Antimicrobial Drugs

Mononuclear Polypyridylruthenium(II) Complexes with High Membrane Permeability in Gram-Negative Bacteria—in particular *Pseudomonas aeruginosa*

Anil K. Gorle,[a] Marshall Feterl,[b, c] Jeffrey M. Warner,[b, c] Sebastian Primrose,[b] Constantin C. Constantinoiu,[b] F. Richard Keene,*[c, d, e] and J. Grant Collins*[a]

Abstract: Ruthenium(II) complexes containing the tetradentate ligand bis[4(4′-methyl-2,2′-bipyridyl)]-1,*n*-alkane ("bb_n"; $n=10$ and 12) have been synthesised and their geometric isomers separated. All $[Ru(phen)(bb_n)]^{2+}$ (phen = 1,10-phenanthroline) complexes exhibited excellent activity against Gram-positive bacteria, but only the *cis*-α-$[Ru(phen)(bb_{12})]^{2+}$ species showed good activity against Gram-negative species. In particular, the *cis*-α-$[Ru(phen)(bb_{12})]^{2+}$ complex was two to four times more active than the *cis*-β-$[Ru(phen)(bb_{12})]^{2+}$ complex against the Gram-negative strains. The *cis*-α- and *cis*-β-$[Ru(phen)(bb_{12})]^{2+}$ complexes readily accumulated in the bacteria but, significantly, showed the highest level of uptake in *Pseudomonas aeruginosa*. Furthermore, the accumulation of the *cis*-α- and *cis*-β-$[Ru(phen)(bb_{12})]^{2+}$ complexes in *P. aeruginosa* was considerably greater than in *Escherichia coli*. The uptake of the *cis*-α-$[Ru(phen)(bb_{12})]^{2+}$ complex into live *P. aeruginosa* was confirmed by using fluorescence microscopy. The water/octanol partition coefficients (log *P*) were determined to gain understanding of the relative cellular uptake. The *cis*-α- and *cis*-β-$[Ru(phen)(bb_n)]^{2+}$ complexes exhibited relatively strong binding to DNA ($K_b \approx 10^6\,M^{-1}$), but no significant difference between the geometric isomers was observed.

Introduction

Infectious diseases remain a leading cause of death worldwide and a developing resistance to antimicrobial drugs is a significant threat to humans.[1] The World Health Organization has identified antimicrobial resistance as one of the most important problems that affects human health.[2] Although there has been modest success in the development of new drugs against Gram-positive bacteria, the therapeutic options for Gram-negative species are extremely limited.[3,4] Furthermore, there are very few drugs for Gram-negative species in the development pipeline. Of the Gram-negative species, the Infectious Diseases Society of America noted that infections caused by *Pseudomonas aeruginosa* were emerging as a particular worldwide concern.[1] Indeed, *P. aeruginosa* is responsible for 10–15% of nosocomial (hospital-acquired) infections worldwide.[5] *P. aeruginosa* is naturally resistant to antimicrobial agents due to the low permeability of its outer membrane,[6,7] which limits the movement of small molecules into the cell for all Gram-negative bacteria. However, this effect is particularly significant for *P. aeruginosa*, in which the outer membrane permeability is ten- to 100-fold lower than, for example, that of *Escherichia coli*.[8]

Transition-metal complexes in general, and ruthenium(II) complexes in particular, have been studied for their use as antimicrobial agents.[9–18] A variety of mononuclear ruthenium complexes have shown good activity against Gram-positive bacteria, but generally poor activity against Gram-negative species.[14–16] In an attempt to extend and enhance the activity of polypyridylruthenium(II) complexes, particularly against current drug-resistant bacterial strains, we have examined the antimicrobial properties of di-, tri-, and tetra-nuclear polypyridylruthenium(II) complexes, in which the metal centres are linked by the bis[4(4′-methyl-2,2′-bipyridyl)]-1,*n*-alkane ligand (bb_n; Figure 1).[17,18] These oligonuclear complexes have shown excellent activity against drug-sensitive Gram-positive bacterial strains such as *Staphylococcus aureus* and maintained the activity against drug-resistant strains such as methicillin-resistant

[a] *A. K. Gorle, Prof. J. G. Collins*
School of Physical, Environmental and Mathematical Sciences
University of New South Wales, Australian Defence Force Academy
Canberra, ACT 2600 (Australia)
E-mail: g.collins@adfa.edu.au

[b] *Dr. M. Feterl, Prof. J. M. Warner, S. Primrose, Dr. C. C. Constantinoiu*
College of Public Health
Medical and Veterinary Sciences, James Cook University
Townsville, QLD, 4811 (Australia)

[c] *Dr. M. Feterl, Prof. J. M. Warner, Prof. F. R. Keene*
Centre for Biodiscovery and Molecular Development of Therapeutics
James Cook University
Townsville, QLD 4811 (Australia)

[d] *Prof. F. R. Keene*
College of Science, Technology and Engineering
James Cook University, Townsville, QLD 4811 (Australia)

[e] *Prof. F. R. Keene*
School of Physical Sciences, University of Adelaide
Adelaide, SA 5005 (Australia)
E-mail: richard.keene@adelaide.edu.au

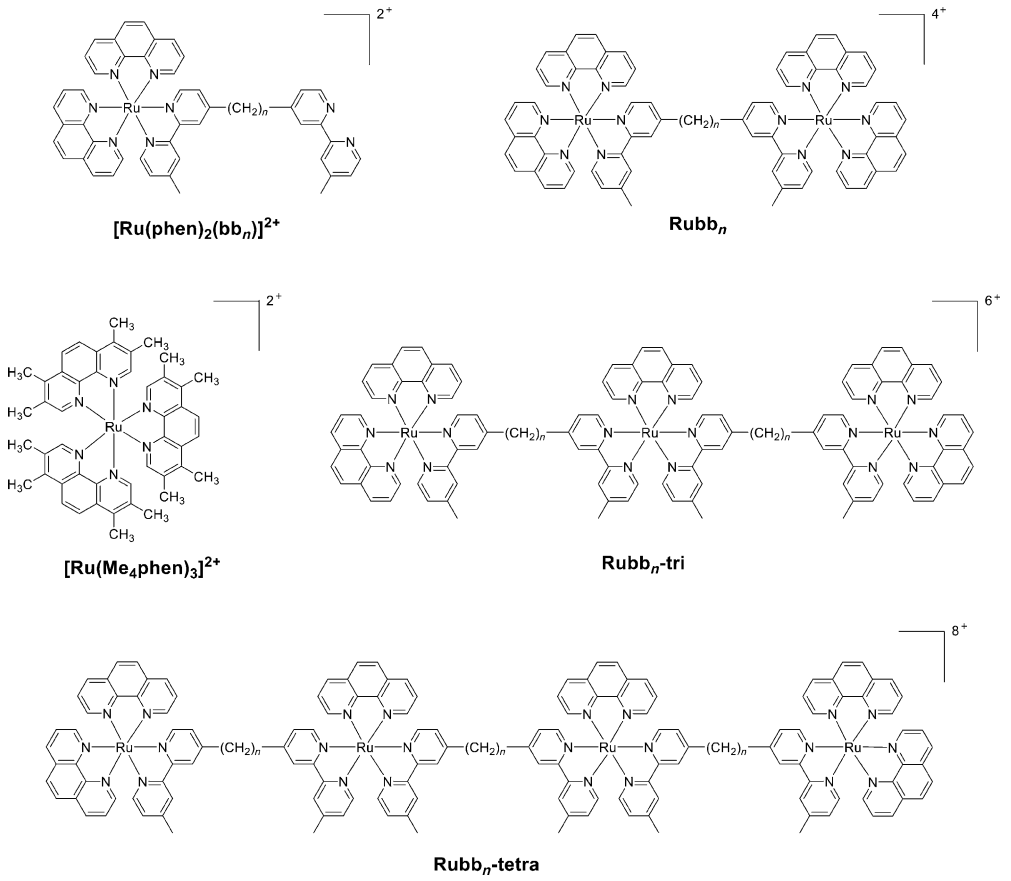

Figure 1. Structure of $[Ru(phen)_2(bb_n)]^{2+}$, $Rubb_n$, $[Ru(Me_4phen)_3]^{2+}$, $Rubb_n$-tri, and $Rubb_n$-tetra complexes.

S. aureus (MRSA).[17,18] However, the ruthenium complexes exhibited relatively poor activity against *P. aeruginosa*, although they showed good activity against the Gram-negative strain *E. coli*.[17,18]

In previous studies, we have demonstrated that the mononuclear complex $[Ru(Me_4phen)_3]^{2+}$ (Me_4phen = 3,4,7,8-tetramethyl-1,10-phenanthroline) and dinuclear complexes $Rubb_{12}$ and $Rubb_{16}$, which showed excellent activity towards Gram-positive bacteria, readily accumulated in the bacterial cell.[19] However, these mono- and dinuclear complexes do not readily accumulate in *P. aeruginosa* and show low activity towards this species. To improve the cellular uptake and thereby increase the activities of ruthenium complexes against *P. aeruginosa* while maintaining activity against Gram-positive strains, we recently studied the antimicrobial properties of the inert tri- and tetranuclear polypyridylruthenium(II) complexes $Rubb_n$-tri and $Rubb_n$-tetra.[18] The trinuclear and tetranuclear complexes were more active than the dinuclear complexes against the Gram-positive strains. However, although the cellular uptake of the tri- and tetranuclear complexes into *P. aeruginosa* was vastly improved relative to the dinuclear complexes, no improvement in activity was observed.[18] Taken together, these results suggest that *P. aeruginosa* is more sensitive to the mononuclear complexes than to complexes with higher nuclearity. However, simply increasing the lipophilicity of a mononuclear complex does not necessarily improve the cellular uptake. We have previously demonstrated that the uptake of the $[Ru(phen)_2(bb_7)]^{2+}$ complex ($\log P = -0.7$) in *P. aeruginosa* is not significantly improved relative to the $[Ru(Me_4phen)_3]^{2+}$ ion and is actually lower than the less lipophilic dinuclear complex $Rubb_{16}$ ($\log P = -1.9$).[19]

In an attempt to increase the cellular accumulation of mononuclear ruthenium complexes in *P. aeruginosa*, we sought to utilise the lipophilicity of the bb_n ligand; however, rather than having a dangling bb_n chain, we aimed to use bb_n as a tetradentate ligand to produce a $[Ru(phen)(bb_n)]^{2+}$ ion (the two accessible geometric isomeric forms of the complex *cis*-α-$[Ru(phen)(bb_n)]^{2+}$ and *cis*-β-$[Ru(phen)(bb_n)]^{2+}$ are shown in Figure 2a,b). Although the $[Ru(phen)(bb_n)]^{2+}$ ion would be expected to have a similar or greater lipophilicity than the most active mononuclear complex (i.e., $[Ru(Me_4phen)_3]^{2+}$), the two isomeric forms have a different physical shape and hence could interact with biological receptors in a different manner.

Herein, we describe the synthesis of these $[Ru(phen)(bb_n)]^{2+}$ complexes, the separation of their geometric isomers, and our examination of their antimicrobial activity, cellular accumulation in four bacteria and their affinity for DNA. In addition, fluorescence microscopy was used to examine the uptake of the *cis*-α-$[Ru(phen)(bb_{12})]^{2+}$ ion into live *P. aeruginosa*. The results indicate that the *cis*-α- and *cis*-β-$[Ru(phen)(bb_{12})]^{2+}$ complexes readily accumulate in *P. aeruginosa*. Furthermore, the symmetric isomer *cis*-α-$[Ru(phen)(bb_{12})]^{2+}$ showed good activity

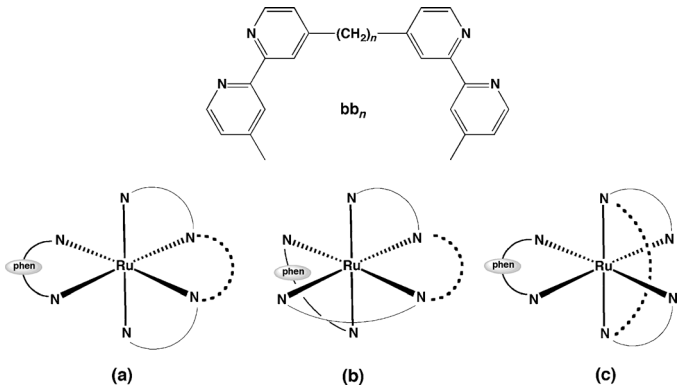

Figure 2. The ligand bb_n and the possible isomeric forms of the mononuclear complex $[Ru(phen)(bb_n)]^{2+}$ with bb_n as a tetradentate ligand: a) *cis*-α isomer, b) *cis*-β isomer, and c) a form in which the central polymethylene chain spans the *trans* positions. The isomers shown in (a) and (c) have C_2 point-group symmetry, whereas the *cis*-β isomer is asymmetric (C_1).

against *P. aeruginosa* and was more active than the corresponding unsymmetric *cis*-β-$[Ru(phen)(bb_{12})]^{2+}$ isomer.

Results

Synthesis

The synthesis of a series of mononuclear $[Ru(phen)(bb_n)]^{2+}$ complexes containing the flexible bb_n ligand has been achieved in good yields (Scheme 1). The ruthenium complexes were prepared by heating *cis*,*cis*-$[RuCl_2(DMSO)_2(phen)]$ (DMSO = dimethyl sulfoxide) to reflux with the bb_n ligand in ethylene glycol and was purified by cation-exchange chromatography on a SP Sephadex C-25 column with aqueous sodium chloride as the eluent, followed by recrystallisation from acetonitrile/diethyl ether. The *cis*-α and *cis*-β geometrical isomers of the mononuclear $[Ru(phen)(bb_n)]^{2+}$ complexes were separated by cation-exchange chromatography on a SP Sephadex C-25 column with sodium toluene-4-sulfonate as the eluent and a column length of approximately 1 metre. The complexes were characterised by using microanalysis, NMR spectroscopy and high-resolution electrospray ionisation (ESI) mass spectrometry. Although the $[Ru(phen)(bb_n)]^{2+}$ complexes were prepared so that their antimicrobial activity could be examined relative to the previously reported $Rubb_n$ and $[Ru(Me_4phen)_3]^{2+}$ complexes, these complexes could also be useful as DNA-binding probes.[20–23]

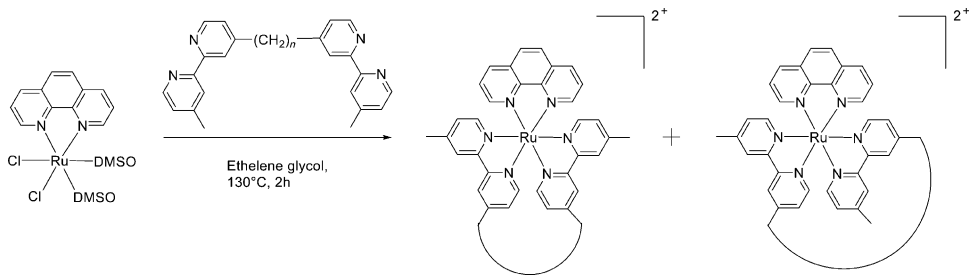

Scheme 1. Synthesis of $[Ru(phen)(bb_n)]^{2+}$ complexes containing the bb_n ligand.

Geometric isomers

The phen ligand places constraints upon the coordination disposition of the bb_n ligand as a tetradentate ligand, and there are actually three possible geometric isomers for the $[Ru(phen)(bb_n)]^{2+}$ complexes; namely, the symmetrical *cis*-α and unsymmetrical *cis*-β forms (Figure 2a,b, respectively) and an additional "symmetrical" isomer in which the pyridine groups of two 2,2′-bipyridine moieties bearing the bridging methylene chain are coordinated in *trans* positions around the metal centre (Figure 2c). The ability of a bidentate ligand containing a polymethylene chain ($n \geq 10$) to function as a *trans*-spanning chelate ring has been reported,[24] but is not common. Only one of the two possible symmetrical isomers *cis*-α-$[Ru(phen)(bb_n)]^{2+}$ was observed in the ^1H NMR spectrum of the reaction mixture, thus indicating that the highly strained (based upon molecular modelling) alternative symmetrical isomer with the *trans*-spanning central ring was not formed, presumably because of steric crowding. Molecular models of the two geometric isomers that were formed are shown in Figure 3.

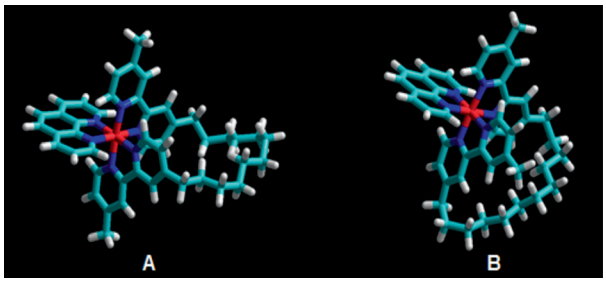

Figure 3. Molecular models of the isomers *cis*-α-$[Ru(phen)(bb_{12})]^{2+}$ (A) and *cis*-β-$[Ru(phen)(bb_{12})]^{2+}$ (B), produced by using the HyperChem program. Ru = red, C = cyan, H = white, N = blue.

The structures of the *cis*-α and unsymmetrical *cis*-β isomers were confirmed by NMR spectroscopic analysis. Only one symmetrical set of resonances is observed for both the phen and bb_n aromatic protons for the *cis*-α-$[Ru(phen)(bb_n)]^{2+}$ structure (Figure 4C). Alternatively, a near doubling of the number of resonances from the aromatic protons is observed for the unsymmetrical *cis*-β-$[Ru(phen)(bb_n)]^{2+}$ structure (Figure 4B). The identity of the symmetric ruthenium complex was unambiguously determined by comparing ROE crosspeaks in ROESY spectra of the ruthenium complex with interproton distances obtained from molecular models of the *cis*-α-$[Ru(phen)(bb_n)]^{2+}$ structure.

The relative proportions of the *cis*-α and *cis*-β isomers in the

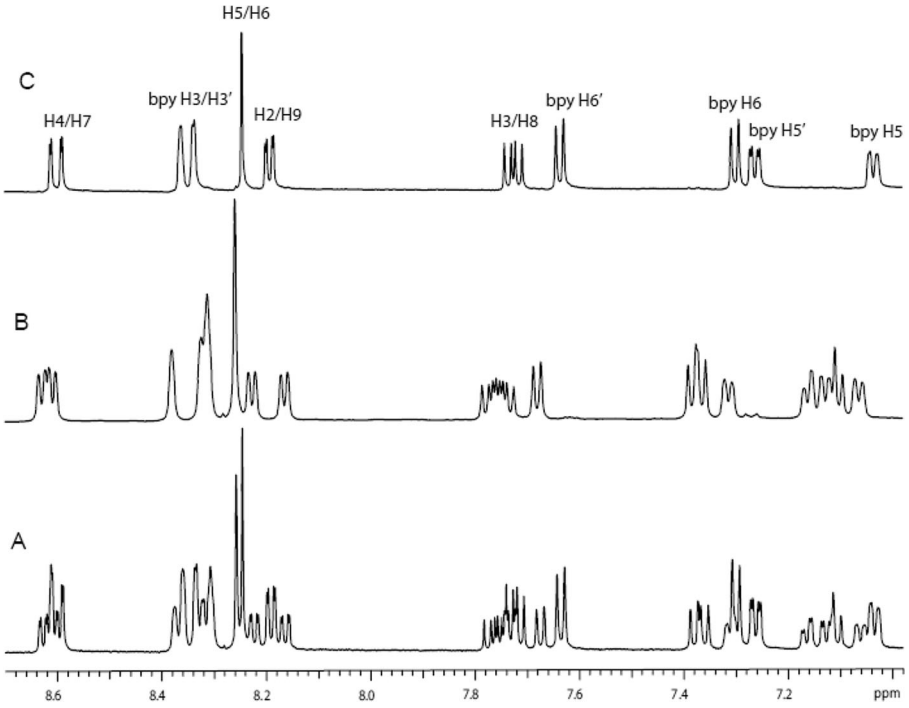

Figure 4. Aromatic region of the ^{1}H NMR spectra of the $[Ru(phen)(bb_{12})]^{2+}$ complexes in CD_3CN. A) mixture of the *cis*-α and *cis*-β isomers, B) *cis*-β isomer and C) *cis*-α isomer.

synthesis was dependent upon both the number of added equivalents of the bb_n ligand and the number of methylene groups in the bb_n ligand. For $[Ru(phen)(bb_{12})]^{2+}$, the addition of four equivalents of the bb_{12} ligand to *cis*,*cis*-$[RuCl_2(DMSO)_2(phen)]$ resulted in a 1:1 ratio of *cis*-α/*cis*-β, whereas when only 1.2 equivalents of bb_{12} ligand were used, the observed ratio was 1:2. For $[Ru(phen)(bb_{10})]^{2+}$, 1.2 equivalents of bb_{10} resulted in a 1:1.5 ratio of *cis*-α/*cis*-β.

Antimicrobial activity

The minimum inhibitory concentration (MIC) for the $[Ru(phen)(bb_n)]^{2+}$ complexes against four bacterial strains (i.e., *S. aureus*, MRSA, *E. coli*, and *P. aeruginosa*) were determined (the results are summarised in Table 1). The results demonstrate that the *cis*-α-$[Ru(phen)(bb_{12})]^{2+}$ and *cis*-β-$[Ru(phen)(bb_{12})]^{2+}$ complexes have significant antimicrobial activity against both classes of bacteria, but are more active against the Gram-positive than the Gram-negative species. Of particular note, the *cis*-α-$[Ru(phen)(bb_{12})]^{2+}$ complex is two–four times more active than the *cis*-β-$[Ru(phen)(bb_{12})]^{2+}$ isomer against the Gram-negative species, but both isomers show equal activity against the Gram-positive bacteria. The $[Ru(phen)(bb_{12})]^{2+}$ complexes are two–four times more active than the corresponding $[Ru(phen)(bb_{10})]^{2+}$ species. Although the *cis*-α-$[Ru(phen)(bb_{12})]^{2+}$ complex exhibited similar activity to that previously reported for $[Ru(Me_4phen)_3]^{2+}$, dinuclear, trinuclear, and tetranuclear ruthenium complexes against the Gram-positive bacteria and *E. coli*, it was more active against *P. aeruginosa*.[16,18] In particular, it was four times more active than the $[Ru(Me_4phen)_3]^{2+}$ complex.

Lipophilicity (log *P*)

Lipophilicity is one factor that affects the biological activity of any metal complex because lipophilicity is generally correlated to the capacity of the drug to penetrate through the cell membrane. The standard octanol/water partition coefficient (log *P*) was determined for the $[Ru(phen)(bb_n)]^{2+}$ and $[Ru(Me_4phen)_3]^{2+}$ complexes (the results are summarised in Table 2). As expected, the $[Ru(phen)(bb_{12})]^{2+}$ isomers are more lipophilic than their $[Ru(phen)(bb_{10})]^{2+}$ analogues. More significantly, the $[Ru(phen)(bb_{12})]^{2+}$ isomers are more lipophilic than the $[Ru(Me_4phen)_3]^{2+}$ complex, are of similar lipophilicity to $Rubb_{12}$-tri, and are less lipophilic than the $[Ru(phen)_2(bb_7)]^{2+}$ complex.

Table 1. MIC values (μg mL^{-1}) for the ruthenium complexes after 16–18 hours of incubation against Gram-positive and Gram-negative bacterial strains.

	Gram positive		Gram negative	
Complexes	*S. aureus*	MRSA	*E. coli*	*P. aeruginosa*
cis-α-$[Ru(phen)(bb_{10})]^{2+}$	1	16	32	32
cis-β-$[Ru(phen)(bb_{10})]^{2+}$	1	16	32	32
cis-α-$[Ru(phen)(bb_{12})]^{2+}$	0.5	4	8	8
cis-β-$[Ru(phen)(bb_{12})]^{2+}$	0.5	4	16	32
$[Ru(Me_4phen)_3]^{2+}$	0.5	4	8	32
$[Ru(phen)_2(bb_7)]^{2+}$	4	16	16	32
$[Ru(phen)_2(bb_{16})]^{2+}$	16	16	64	64
ampicillin	1	>128	4	>128
gentamicin	<0.5	32	0.5	1

Cellular accumulation

The cellular accumulations of the *cis*-α-$[Ru(phen)(bb_{12})]^{2+}$ and *cis*-β-$[Ru(phen)(bb_{12})]^{2+}$ complexes in *S. aureus*, MRSA, *E. coli* and *P. aeruginosa* were determined by measuring the concentration of the ruthenium complex that remained in the culture supernatant after removing the bacteria by centrifugation. The concentration of the ruthenium complex in the supernatant was calculated from an absorbance-calibration curve obtained by adding known concentrations of the ruthenium complex to a blank supernatant. As the absorbance of the ruthenium

Table 2. Octanol/water partition coefficients (log *P*) for the ruthenium complexes.

Metal complex	Charge	log *P*
$[Ru(Me_4phen)_3]^{2+}$	+2	−1.35
$[Ru(phen)_2(bb_7)]^{2+}$[a]	+2	−0.7
cis-α-$[Ru(phen)(bb_{10})]^{2+}$	+2	−1.2
cis-β-$[Ru(phen)(bb_{10})]^{2+}$	+2	−1.4
cis-α-$[Ru(phen)(bb_{12})]^{2+}$	+2	−0.9
cis-β-$[Ru(phen)(bb_{12})]^{2+}$	+2	−1.0
$Rubb_{12}$[b]	+4	−2.9
$Rubb_{16}$[b]	+4	−1.9
$Rubb_{10}$-tri[b]	+6	−1.3
$Rubb_{12}$-tri[b]	+6	−1.0
$Rubb_{16}$-tri[b]	+6	−0.8
$Rubb_{10}$-tetra[b]	+8	−1.7
$Rubb_{12}$-tetra[b]	+8	−1.6
$Rubb_{16}$-tetra[b]	+8	−0.95

[a] Results from ref. [16]. [b] Results from ref. [18].

complexes varied with the different broths and supernatants for each bacterial strain, a calibration curve was determined for each complex in the supernatant of each bacterial strain. Figures 5 and 6 show the cellular accumulation of the *cis*-α-$[Ru(phen)(bb_{12})]^{2+}$ and *cis*-β-$[Ru(phen)(bb_{12})]^{2+}$ complexes into the bacteria after 45 minutes and as a function of time for up to two hours of incubation. The *cis*-α- and *cis*-β-$[Ru(phen)(bb_{12})]^{2+}$ isomers exhibited higher levels of accumulation in *P. aeruginosa* than with *E. coli*, unlike other ruthenium complexes (mono- and oligonuclear) in which accumulation in *E. coli* was consistently either similar to or greater than that in *P. aeruginosa*.[18,19] Furthermore, both the *cis*-α and *cis*-β isomers of $[Ru(phen)(bb_{12})]^{2+}$ exhibited much higher levels of accumulation than either the $[Ru(Me_4phen)_3]^{2+}$ or $[Ru(phen)_2(bb_7)]^{2+}$ complexes with *P. aeruginosa* (Figure 6), but accumulated to similar levels with the trinuclear and tetranuclear $Rubb_n$ complexes in this bacterium.[18]

Another interesting difference in the accumulation of the *cis*-α and *cis*-β isomers of $[Ru(phen)(bb_{12})]^{2+}$ in *P. aeruginosa* was the observed decrease in accumulation over longer time points relative to the observed increase in the accumulation of the $[Ru(Me_4phen)_3]^{2+}$ and $[Ru(phen)_2(bb_7)]^{2+}$ complexes over two hours (Figure 6).

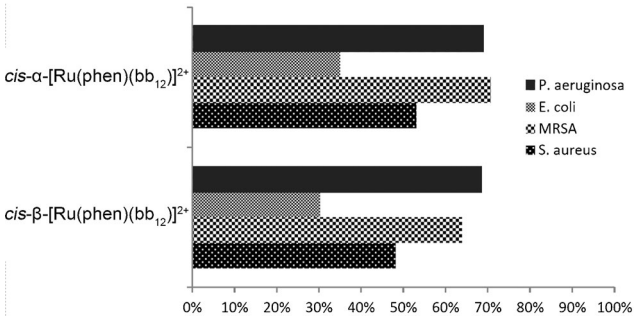

Figure 5. Cellular uptake of the *cis*-α-$[Ru(phen)(bb_{12})]^{2+}$ and *cis*-β-$[Ru(phen)(bb_{12})]^{2+}$ complexes into bacteria after incubation for 45 minutes. The experimental error in all cases is $\leq 5\%$.

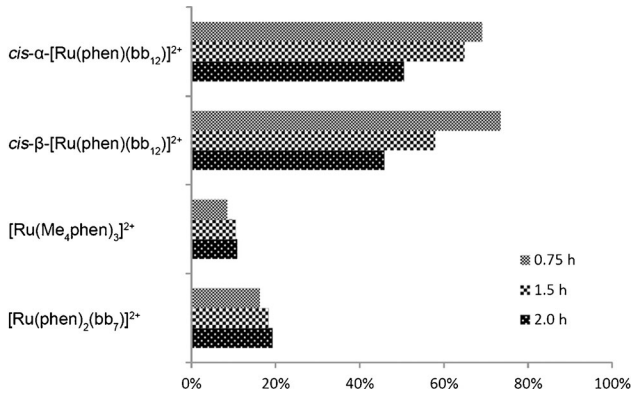

Figure 6. Cellular uptake of the *cis*-α-$[Ru(phen)(bb_{12})]^{2+}$, *cis*-β-$[Ru(phen)(bb_{12})]^{2+}$, $[Ru(Me_4phen)_3]^{2+}$ and $[Ru(phen)_2(bb_7)]^{2+}$ complexes into *P. aeruginosa* after incubation for 0.75, 1.5 and 2.0 h. The experimental error is $\leq 5\%$.

Epifluorescence microscopy

The accumulation of the *cis*-α-$[Ru(phen)(bb_{12})]^{2+}$ complex in *P. aeruginosa* was examined by epifluorescence microscopy to confirm the cellular uptake of the ruthenium complexes. Figure 7 shows an epifluorescence microscopy image of *P. aeruginosa* incubated with *cis*-α-$[Ru(phen)(bb_{12})]^{2+}$ at 8 μg mL^{-1} (MIC) for two hours. Figure 7 shows that the ruthenium complex is taken up by the bacterium at MIC concentrations. Although the resolution is low, due to the small size of *P. aeruginosa*, the results suggest that the ruthenium complex is not localised within the bacterium (see the lower panel of Figure 7), with the *cis*-α-$[Ru(phen)(bb_{12})]^{2+}$ complex appearing to be evenly distributed throughout the cytoplasm. However, when *P. aeruginosa* was incubated with the ruthenium complex at 4×MIC, which resulted in a stronger signal and greater contrast, the results suggest that the ruthenium complex may be

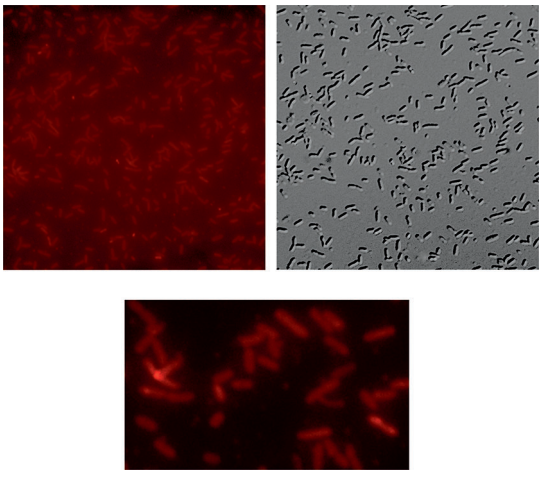

Figure 7. Epifluorescence microscopy images of a *P. aeruginosa* sample incubated with 8 μg mL^{-1} *cis*-α-$[Ru(phen)(bb_{12})]^{2+}$ for 2 h. The fluorescence microscopy images show phosphorescence (top, right), phase contrast (top, left), and expansion of the ruthenium complex phosphorescence (bottom).

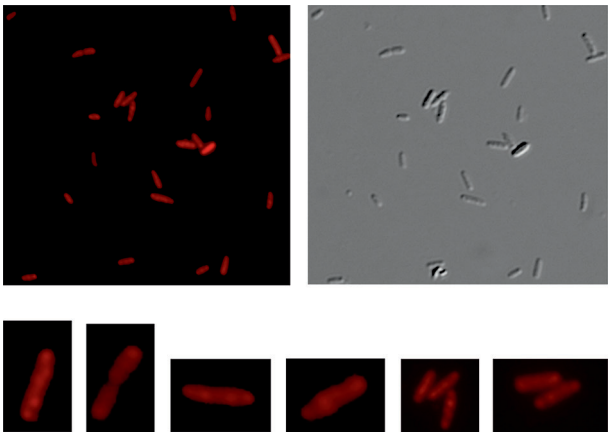

Figure 8. Epifluorescence microscopy images of a *P. aeruginosa* sample incubated with 32 μg mL^{-1} *cis*-α-[Ru(phen)(bb$_{12}$)]$^{2+}$ for 2 h. The fluorescence microscopy images show phosphorescence (top, right), phase contrast (top, left), and expansion of the ruthenium complex phosphorescence (bottom).

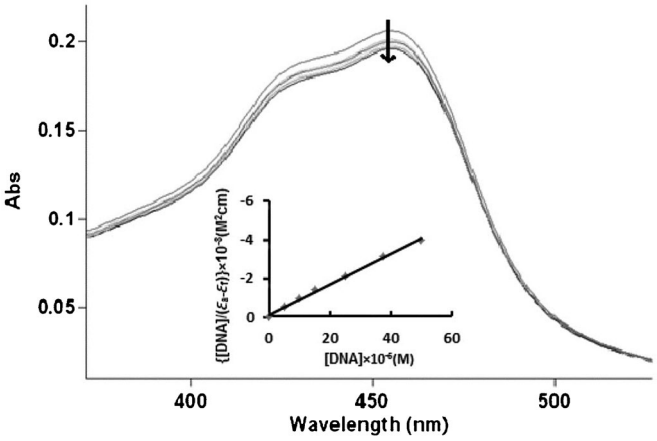

Figure 9. UV absorption spectra of the *cis*-α-[Ru(phen)(bb$_{12}$)]$^{2+}$ ion in the absence and presence of CT-DNA with increasing DNA/complex ratios from 0:1 to 2:1. The arrow shows the changes upon increasing concentrations of CT-DNA. Inset: plot of [DNA]/($\varepsilon_a-\varepsilon_f$) versus [DNA].

localised to a small extent in the bacterium (Figure 8). The phosphorescence[25] from the *cis*-α-[Ru(phen)(bb$_{12}$)]$^{2+}$ complex appears to be slightly stronger at the cell poles, in a similar manner to observations in an earlier study, with the dinuclear complex Rubb$_{16}$ in *E. coli*.[26] However, unlike the results observed with Rubb$_{16}$, in which the dinuclear complex very selectively localised at the cell poles and at particular points in the middle of the cells,[26] the selective localisation with the *cis*-α-[Ru(phen)(bb$_{12}$)]$^{2+}$ complex appears to be much less pronounced. In the study with *E. coli*, it was concluded that the Rubb$_{16}$ complex selectively bound the RNA of the ribosomes, with the unbound chromosomal DNA occupying the remainder of the cytoplasm.[26] Based upon the comparison of the fluorescence microscopy analysis of the Rubb$_{16}$ and *cis*-α-[Ru(phen)(bb$_{12}$)]$^{2+}$ complexes, it is tentatively concluded that the *cis*-α-[Ru(phen)(bb$_{12}$)]$^{2+}$ complex does not show a significant selectivity for RNA relative to DNA.

Interaction with DNA

The binding of the [Ru(phen)(bb$_n$)]$^{2+}$ complexes to calf-thymus (CT)-DNA was examined by UV/Vis spectroscopic analysis to determine if the *cis*-α-[Ru(phen)(bb$_n$)]$^{2+}$ isomers bound DNA with a greater affinity than the *cis*-β-[Ru(phen)(bb$_n$)]$^{2+}$ analogues. With increasing concentrations of DNA, the absorbance of the *cis*-α-[Ru(phen)(bb$_n$)]$^{2+}$ and *cis*-β-[Ru(phen)(bb$_n$)]$^{2+}$ complexes at $\lambda = 454$ nm decreased by 6–10% (for example, see Figure 9). The binding constant (K_b) of the ruthenium complexes with CT-DNA was calculated by using the standard equation [Eq. (1)] and the ratio of the slope to the intercept in plots of [DNA]/($\varepsilon_a-\varepsilon_f$) versus [DNA].[27]

$$[\mathrm{DNA}]/(\varepsilon_a-\varepsilon_f) = [\mathrm{DNA}]/(\varepsilon_b-\varepsilon_f) + 1/K_b(\varepsilon_b-\varepsilon_f) \quad (1)$$

where ε_a, ε_b and ε_f are the apparent, bound, and free molar absorption coefficients of the ruthenium complexes, respectively; [DNA] is the CT-DNA concentration; and K_b is the binding constant.

All [Ru(phen)(bb$_n$)]$^{2+}$ complexes showed relatively strong binding to CT-DNA, with binding constants of approximately 1×10^6 M^{-1} (Table 3). However, no significant differences in the DNA binding affinities between the *cis*-α-[Ru(phen)(bb$_n$)]$^{2+}$ and *cis*-β-[Ru(phen)(bb$_n$)]$^{2+}$ isomers were observed. In addition, the [Ru(Me$_4$phen)$_3$]$^{2+}$ ion bound with similar or even slightly higher affinity than the [Ru(phen)(bb$_n$)]$^{2+}$ complexes.

Table 3. The CT-DNA binding constants (K_b) of the [Ru(phen)(bb$_n$)]$^{2+}$ and [Ru(Me$_4$phen)$_3$]$^{2+}$ complexes

Complex	K_b [M^{-1}]
[Ru(Me$_4$phen)$_3$]$^{2+}$	2.0×10^6
cis-α-[Ru(phen)(bb$_{10}$)]$^{2+}$	1.0×10^6
cis-β-[Ru(phen)(bb$_{10}$)]$^{2+}$	1.1×10^6
cis-α-[Ru(phen)(bb$_{12}$)]$^{2+}$	8.0×10^5
cis-β-[Ru(phen)(bb$_{12}$)]$^{2+}$	5.0×10^5

Discussion

Gram-negative bacteria have an additional membrane relative to Gram-positive species, and this second outer membrane functions as an effective barrier to antimicrobial drugs. One reason for the reduced permeability is that the outer leaflet of the outer membrane is composed of lipopolysaccharide (LPS) rather than the glycerophospholipids usually found in biological membranes.[28] LPSs contain six or seven fatty-acid chains, rather than the two chains in glycerophospholipids.[27] As a consequence, a LPS-based bilayer has a low fluidity, hence even hydrophobic drugs partition poorly into the hydrophobic section of the bilayer. Furthermore, although many Gram-negative bacteria have high-permeability porins (proteins that produce diffusion channels across membranes), *P. aeruginosa* has only low-efficiency porins suitable for small molecules.[28,29] Conse-

quently, the development of molecules that can easily cross the membrane of *P. aeruginosa* is an important aspect in the development of new antimicrobial agents.

We, together with other researchers, have previously shown that certain types of polypyridylruthenium(II) complex exhibit good antimicrobial activity against Gram-positive bacteria, but only variable activity against Gram-negative species.[14–18] In particular, very few ruthenium(II) complexes, or complexes of other transition metals, have shown good activity against *P. aeruginosa*, which is a bacterium of current concern.[1,5] In previous studies, we have demonstrated that the mononuclear complexes $[Ru(Me_4phen)_3]^{2+}$ or $[Ru(phen)_2(bb_7)]^{2+}$ do not readily accumulate in *P. aeruginosa* and only exhibit modest antimicrobial activities against this bacterium.[19] Alternatively, trinuclear and tetranuclear complexes readily accumulate in *P. aeruginosa*, but also only exhibit modest activities against this species.[18] The results of this study are significant in terms of the development of new antimicrobial agents in two ways: 1) the *cis*-α- and cis-β-$[Ru(phen)(bb_{12})]^{2+}$ complexes accumulate readily in *P. aeruginosa* (and to a considerably greater extent than in *E. coli*), and the *cis*-α-$[Ru(phen)(bb_{12})]^{2+}$ complex shows good activity against *P. aeruginosa*, albeit still with lower activity than with Gram-positive species; and 2) more generally, this study suggests that, in the future development of metal-based antimicrobial agents, it could be advantageous to increase lipophilicity by incorporating alkane groups in an expanded chelate ring, such as in the *cis*-α-$[Ru(phen)(bb_{12})]^{2+}$ complex, rather than through the addition of an alkyl chain or methyl groups on aromatic ligands.

The $[Ru(phen)(bb_n)]^{2+}$ complexes can be synthesised in good yield and the geometric isomers easily separated. The $[Ru(phen)(bb_n)]^{2+}$ complexes are slightly more lipophilic than the $[Ru(Me_4phen)_3]^{2+}$ complex, but less lipophilic than the $[Ru(phen)_2(bb_7)]^{2+}$ complex. However, the $[Ru(phen)(bb_n)]^{2+}$ complexes accumulate in *P. aeruginosa* to a considerably greater extent than in either the $[Ru(Me_4phen)_3]^{2+}$ or $[Ru(phen)_2(bb_7)]^{2+}$ complexes. This outcome suggests that the differences in cellular uptake between these ruthenium complexes is not primarily related to lipophilicity, as judged by log*P*, but due to other structural characteristics that affect membrane permeability.

For the *cis*-α- and cis-β-$[Ru(phen)(bb_{12})]^{2+}$ isomers, the level of cellular accumulation in *P. aeruginosa* initially rose to high levels over 45 minutes, but then decreased to some extent over the next 75 minutes. Alternatively, although the initial accumulation was considerably less for the $[Ru(Me_4phen)_3]^{2+}$ and $[Ru(phen)_2(bb_7)]^{2+}$ complexes than that observed with the *cis*-α- and cis-β-$[Ru(phen)(bb_{12})]^{2+}$ isomers, no decrease in accumulation was observed at longer time points up to two hours. Although further studies are required, the results tentatively suggest that *P. aeruginosa* may be able to induce an effective efflux pump against the *cis*-α- and cis-β-$[Ru(phen)(bb_{12})]^{2+}$ complexes.

It is not clear why the *cis*-α-$[Ru(phen)(bb_{12})]^{2+}$ complex is more active than the *cis*-β-$[Ru(phen)(bb_{12})]^{2+}$ complex against *P. aeruginosa* because both isomers accumulated to a similar degree in the bacterium. Previous studies have demonstrated the dinuclear and oligonuclear $Rubb_n$ complexes target DNA and RNA in bacterial and eukaryotic cells.[26,30] Although further studies at higher magnification are required, the results from the initial epifluorescence microscopy study suggests that, unlike the dinuclear ruthenium complex $Rubb_{16}$, which shows a high degree of selectivity for ribosomes (RNA), the *cis*-α isomer binds chromosomal DNA with a similar affinity relative to ribosomal RNA. However, the results of the DNA binding studies for the $[Ru(phen)(bb_n)]^{2+}$ complexes suggest that the binding affinity of the nucleic acids is not likely to be the explanation of the greater activity of *cis*-α-$[Ru(phen)(bb_{12})]^{2+}$ relative to *cis*-β-$[Ru(phen)(bb_{12})]^{2+}$. Although the overall DNA (and potentially RNA) binding affinities are similar, it is probable that the biological consequences of DNA binding could be different (e.g., through different specific high affinity sites), thereby resulting in different antimicrobial activities.

Conclusion

The results of this study indicate that the ruthenium(II) complex *cis*-α-$[Ru(phen)(bb_{12})]^{2+}$ can accumulate readily in *P. aeruginosa*, to a far greater extent than in *E. coli*, and exhibits good antimicrobial activity against either of the bacteria. Our results suggest that the structural differences between the *cis*-α-$[Ru(phen)(bb_{12})]^{2+}$ complex and the mononuclear $[Ru(Me_4phen)_3]^{2+}$ and $[Ru(phen)_2(bb_7)]^{2+}$ complexes previously studied are significant in terms of interactions with the outer membrane of *P. aeruginosa*. As a consequence, and given that the structure can be readily modified, it is possible that ruthenium(II) complexes can be customised to particular bacteria. Perhaps, the results of this study suggest a new structural motif for metal-based antimicrobial drugs, thus paving the way forward for the development of new antimicrobial agents for Gram-negative bacteria.

Experimental Section

Physical measurements

^1H and ^{13}C NMR spectra were recorded on a Varian Advance 400 MHz spectrometer at room temperature in D_2O (99.9%, Cambridge Isotope Laboratories (CIL)), $CDCl_3$ (99.8%, CIL), CD_3CN (> 99.8%, Aldrich), or CD_3OD (> 99.8%, Aldrich). UV absorbance was measured on a Jenway 6300 spectrophotometer. Mass-spectroscopic analysis was performed by the RSC Mass Spectrometry Facility (Research School of Chemistry, Australian National University, Canberra). Microanalyses were performed by the Microanalytical Unit (Research School of Chemistry, Australian National University, Canberra).

Materials and methods

Potassium hexafluorophosphate (KPF_6), ammonium hexafluorophosphate (NH_4PF_6) and 1,10-phenanthroline were purchased from Aldrich and used as supplied. Amberlite IRA-402 (chloride form) anion-exchange resin and SP-Sephadex C-25 cation exchanger were obtained from GE Health Care Bioscience. Cation-adjusted Mueller–Hinton broth (CAMHB) was purchased from Fluka (Gillingham, UK). The control antibiotics gentamicin and ampicillin were

purchased from Oxoid (Australia). The syntheses of ligands bb_n ($n=10$, 12 and 16) and *cis*-$[RuCl_2(DMSO)_4]$ were performed according to previously reported methods.[31,32] The complex *cis*,*cis*-$[RuCl_2(DMSO)_2(phen)]$ was prepared as previously described.[33] The ^{1}H NMR spectrum was consistent with that previously reported.

Bacterial strains

All bacterial strains are classified as a C2 risk group and must be handled within a PC2 laboratory. Two *Staphylococcus aureus* (Gram positive) isolates, a methicillin-susceptible *S. aureus* strain (ATCC 25923), a clinical multidrug-resistant MRSA strain (a wild clinical strain from the JCU culture collection) and two Gram-negative isolates *E. coli* (ATCC 25922) and *P. aeruginosa* (ATCC 27853) were used for antimicrobial studies in vitro.

MIC determination

The MIC tests were conducted by using the broth microdilution method in duplicate as outlined by the Clinical and Laboratory Standards Institute (CLSI).[34] The bacteria were grown on Mueller–Hinton agar and suspended in CAMHB growth medium. Bacterial inocula were adjusted to a turbidity equivalent to that of a 0.5 McFarland standard and diluted to a final concentration of 4–8×10^5 cfu mL^{-1}. The tested compounds were dissolved and serially diluted in CAMHB in sterile 96-well flat-bottom plates to a final volume of 100 μL in each well. An equal volume of inocula was added to each well, thus making a final concentration range of the compounds tested, including the control antibiotics gentamicin and ampicillin (Oxoid, Australia), of between 0.25 and 128 μg mL^{-1}. The MIC measurements were recorded after 16–18 h of incubation at 37 °C.

DNA-binding studies

Experiments were carried out in phosphate-buffered saline (PBS) at pH 7.4. The ratio of the UV absorbance of a solution of CT-DNA at $\lambda=260$ and 280 nm was greater than 1.8, thus indicating that the CT-DNA was sufficiently free from protein. The DNA concentration of the stock solution (2.35×10^{-3} M) was determined by UV absorbance by using a molar absorption coefficient of 13300 M^{-1} cm^{-1} per base pair at $\lambda=260$ nm. Absorption titration experiments were carried out by keeping the concentration of the ruthenium complex constant (2.5×10^{-5} M) and varying the CT-DNA concentration from 0 to 5.0×10^{-5} M. Absorbance values were recorded after each successive addition of the solution of CT-DNA.

Cellular uptake

The cellular uptake of the ruthenium complexes was measured by monitoring the UV absorbance of the complexes that remained in the culture supernatant after incubation for various periods of time. Bacterial inocula in the log phase were adjusted to a cell concentration of 1–5×10^7 cfu mL^{-1}. Aliquots (2 mL) of the adjusted inocula were placed in glass culture tubes and the stock solution (330 mg L^{-1}, 50 μL) of the ruthenium complex was added to give a final concentration of 8 mg L^{-1}. Control flasks containing each bacterial suspension (50 mL) were set up as blank samples to obtain UV calibration curves for each complex. Culture tubes and control flasks were incubated with agitation at 150 rpm at 37 °C for 0.75, 1.5 or 2 h. At the end of incubation, the culture tubes were centrifuged (*S. aureus* and MRSA at 6000 *g*; *E. coli* and *P. aeruginosa* at 17000 *g*) at 4 °C for 10 min. Supernatants (1.6 mL) were carefully transferred to 2 mL tubes and the UV absorbance of the remaining ruthenium complex was measured at $\lambda=488$ nm. Aliquots of a stock solution (330 mg L^{-1}; 10, 30, 40, 50 and 65 μL) of each complex were added to aliquots of the supernatant (2 mL) from each control bacterial suspension (untreated with the drug) to acquire a linear correlation chart of the UV concentration for calibration. The uptake of the complexes was calculated by using the calibration curve obtained from the control bacterial aliquots.

Epifluorescence microscopy

Epifluorescence microscopy images were obtained from an epifluorescence microscope (AxioImager.Z1, Zeiss, Germany), equipped with a digital camera (AxioCamMRm, Zeiss, Germany). A *P. aeruginosa* inoculum in the log phase was adjusted to a 0.5 McFarland standard and incubated in CAMHB growth medium containing *cis*-α-$[Ru(phen)(bb_{12})]Cl_2$ (at 8 or 32 μg mL^{-1}; 1 or 4×MIC) for 2 h. After incubation, an aliquot of the bacterial suspension (1 mL) was centrifuged at 6000 *g* at 4 °C for 5 min, and the pellet was washed four times and resuspended in a final volume of 50 μL of PBS solution. A sample of the suspension was prepared for viewing by epifluorescence microscopy. Briefly, the bacteria were dried on Superfrost Plus glass slides (Menzel-Glaser, Germany) and mounted by using mounting media (Vectashield, Vector Laboratories, USA). Slides were examined at 63× magnification with the filter set 45 (Zeiss, Germany; excitation bandpass (BP): $\lambda=560/40$; emission BP: $\lambda=630/75$ nm).

Lipophilicity (log *P*) determination

The partition coefficients (log *P*) were measured using the shake-flask technique. Each ruthenium complex (0.1 mM) was dissolved in the water phase and an equal volume of *n*-octanol was added. The two phases were mutually saturated by shaking overnight at ambient temperature and allowed to separate on standing. The concentration of the metal complex in each phase was determined spectrophotometrically at $\lambda=450$ nm.

Syntheses

$[Ru(phen)(bb_n)](PF_6)_2$: A solution of *cis*,*cis*-$[RuCl_2(DMSO)_2(phen)]$ (200 mg, 0.39 mmol) and the appropriate bb_n ligand (0.47 mmol) in N_2-purged ethylene glycol (35 mL) was heated to 130–140 °C and stirred in an N_2 atmosphere for 2 h. The reaction mixture turned from light green to bright orange during the course of the reaction. The reaction mixture was cooled to room temperature, and water (10 mL) was added to the bright-orange solution, which was then loaded onto a SP Sephadex C-25 cation-exchange column (3×20 cm). The column was washed with water and the desired mononuclear complex was eluted with aqueous 0.3 M NaCl solution. Solid KPF_6 was added to the eluate and the complex was extracted into dichloromethane (2×30 mL). The organic layer was washed with water (20 mL), dried over anhydrous Na_2SO_4 and evaporated to dryness to obtain the PF_6^- salt of the complex. The complex was further purified by recrystallisation from acetonitrile/diethyl ether to obtain a bright-red/orange solid of $[Ru(phen)(bb_n)](PF_6)_2$. Typical yields were approximately 20–25%.

$[Ru(phen)(bb_{12})](PF_6)_2$: ^{1}H NMR characterisation was carried out for the purified geometrical isomers (see below); TOF MS (ESI+): *m/z* 394.16 ($[M-2PF_6]^{2+}$); calcd for $Ru[C_{46}H_{50}N_6]^{2+}$: *m/z* 394.15, 933.27 ($[M-PF_6]^+$); calcd for $Ru[C_{46}H_{50}N_6](PF_6)^+$: *m/z* 933.28; elemental analysis (%) calcd for $C_{46}H_{50}N_6F_{12}P_2Ru$: C 51.3; H 4.68, N 7.8; found: C 51.2; H 4.73, N 8.0.

[Ru(phen)(bb$_{10}$)](PF$_6$)$_2$: ^{1}H NMR characterisation was carried out for the purified geometrical isomers (see below); TOF MS (ESI+): *m/z* 380.15 (for $[M-2PF_6]^{2+}$); calcd for $Ru[C_{44}H_{46}N_6]^{2+}$: *m/z* 380.14; *m/z* 905.24 ($[M-PF_6]^+$); calcd for $Ru[C_{44}H_{46}N_6](PF_6)^+$: *m/z* 905.25; elemental analysis (%) calcd for $C_{44}H_{46}N_6F_{12}P_2Ru$: C 50.3; H 4.42, N 8.0; found: C 50.0; H 4.28, N 8.0.

Separation of geometric isomers

[Ru(phen)(bb$_n$)](PF$_6$)$_2$ (35 mg; $n=10$, 12) was converted into the chloride salt by stirring in methanol with Amberlite IRA-402 (chloride form) anion-exchange resin for 1 h. After removal of the resin by filtration, the methanol filtrate was evaporated and the resultant chloride salt was dissolved in water (20 mL) and loaded onto a SP Sephadex C-25 cation-exchange column (1.5×90 cm). The symmetrical and unsymmetrical isomers were eluted as two separate bands with an aqueous solution of sodium toluene-4-sulfonate (0.075 M) as the eluent. Solid KPF_6 (ca. 150 mg) was added to the eluents and the complexes were extracted into dichloromethane (2×20 mL). The organic layer was washed with water (20 mL), dried over anhydrous Na_2SO_4, and evaporated to dryness to obtain the PF_6^- salt of the complex. The isomers were further purified by recrystallisation from acetonitrile/diethyl ether.

***cis*-α-[Ru(phen)(bb$_{12}$)](PF$_6$)$_2$**: ^{1}H NMR (400 MHz, CD_3CN): $\delta=8.60$ (dd, $J=1.2$, 8.2 Hz, 2H; H4/H7), 8.37 (brs, 2H; bipy3), 8.34 (d, $J=1.5$ Hz, 2H; bipy3′), 8.25 (s, 2H; H5/H6), 8.20 (dd, $J=1.1$, 5.2 Hz, 2H; H2/H9), 7.73 (dd, $J=5.2$, 8.2 Hz, 2H; H3/H8), 7.64 (d, $J=5.7$ Hz, 2H; bipy6′), 7.30 (d, $J=5.7$ Hz, 2H; bipy6), 7.27 (dd, $J=1.7$, 5.8 Hz, 2H; bipy5′), 7.04 (dd, $J=1.0$, 5.8 Hz, 2H; bipy5), 2.84 (t, $J=13.4$ Hz, 4H; CH_2 bipy), 2.48 (s, 6H; CH_3 bipy), 1.66–1.58 (m, 4H; CH_2 bipy), 1.18–1.04 ppm (m, 16H; 8×CH_2).

***cis*-β-[Ru(phen)(bb$_{12}$)](PF$_6$)$_2$**: ^{1}H NMR (400 MHz, CD_3CN): $\delta=8.63$ (dd, $J=1.2$, 4.8 Hz, 1H; H7 (or H4)), 8.61 (dd, $J=1.2$, 4.8 Hz, 1H; H4 (or H7)), 8.38 (brs, 1H; bipy3), 8.32 (brs, 1H; bipy3′), 8.31 (m, 2H; bipy3 and 3′), 8.26 (s, 2H; H5/H6), 8.22 (dd, $J=1.3$, 5.3 Hz, 1H; H2 (or H9)), 8.16 (dd, $J=1.3$, 5.3 Hz, 1H; H9 (or H2)), 7.79–7.72 (m, 2H; H3/H8), 7.68 (d, $J=5.8$ Hz, 1H; bipy6), 7.39–7.35 (m, 2H; bipy6 and 6′), 7.31 (dd, $J=1.7$, 5.4 Hz, 1H; bipy5), 7.16 (m, 1H; bipy6′), 7.14–7.09 (m, 2H; bipy5′), 7.06 (dd, $J=1.2$, 5.6 Hz, 1H; bipy5), 2.90 (t, $J=12.6$ Hz, 2H; CH_2 bipy), 2.86–2.78 (m, 2H; CH_2 bipy), 2.56 (s, 3H; CH_3 bipy), 2.47 (s, 3H; CH_3 bipy), 1.82–1.68 (m, 4H; CH_2 bipy), 1.38–1.18 ppm (m, 16H; 8×CH_2).

***cis*-α-[Ru(phen)(bb$_{10}$)](PF$_6$)$_2$**: ^{1}H NMR (400 MHz, CD_3CN): $\delta=8.61$ (dd, $J=1.2$, 8.2 Hz, 2H; H4/H7), 8.36 (brs, 2H; bipy3), 8.31 (d, $J=1.5$ Hz, 2H; bipy3′), 8.26 (s, 2H; H5/H6), 8.23 (dd, $J=1.1$, 5.2 Hz, 2H; H2/H9), 7.73 (dd, $J=5.2$, 8.3 Hz, 2H; H3/H8), 7.60 (d, $J=5.8$ Hz, 2H; bipy6′), 7.27 (d, $J=5.7$ Hz, 2H; bipy6), 7.23 (dd, $J=1.5$, 5.7 Hz, 2H; bipy5′), 7.03 (dd, $J=1.0$, 5.8 Hz, 2H; bipy5), 2.83 (t, $J=13.1$ Hz, 4H; CH_2 bipy), 2.48 (s, 6H; CH_3 bipy), 1.66–1.53 (m, 4H; CH_2 bipy), 1.16–1.01 ppm (m, 12H; 6×CH_2).

***cis*-β-[Ru(phen)(bb$_{10}$)](PF$_6$)$_2$**: ^{1}H NMR (400 MHz, CD_3CN): $\delta=8.66$–8.61 (m, 2H; H4/H7), 8.33–8.28 (m, 4H; bipy3 and 3′), 8.28 (s, 2H; H5/H6), 8.26–8.22 (m, 2H; H2/H9), 7.80 (m, 1H; H3 (or H8)), 7.75 (m, 1H; H8 (or H3)), 7.64 (d, $J=5.8$ Hz, 1H; bipy6), 7.46 (d, $J=5.7$ Hz, 1H; bipy6′), 7.39 (d, $J=5.6$ Hz, 1H; bipy6), 7.34 (m, 1H; bipy5), 7.22 (dd, $J=1.3$ Hz, 5.9 Hz, 1H; bipy5′), 7.14 (dd, $J=1.1$ Hz, 5.8 Hz, 1H; bipy5′), 7.09 (dd, $J=1.0$ Hz, 5.7 Hz, 1H; bipy5), 6.85 (d, $J=6.0$ Hz, 1H; bipy6′), 2.93–2.86 (m, 2H; CH_2 bipy), 2.84–2.77 (m, 2H; CH_2 bipy), 2.56 (s, 3H; CH_3 bipy), 2.47 (s, 3H; CH_3 bipy), 1.71–1.56 (m, 4H; CH_2 bipy), 1.36–1.10 (m, 12H; 6×CH_2).

Acknowledgements

We wish to thank UNSW Canberra for a scholarship to A.K.G., and for travel support to allow A.K.G. to undertake the microbiological aspects of the study at James Cook University.

Keywords: bioinorganic chemistry · biological activity · cellular uptake · lipophilicity · N ligands · ruthenium

[1] H. W. Boucher, G. H. Talbot, J. S. Bradley, J. E. Edwards Jr, D. Gilbert, L. B. Rice, M. Scheld, B. Spellberg, J. Bartlett, *IDSA Report on Development Pipeline* **2009**, *48*, 1.
[2] WHO Report, 30 April, 2014, see http://www.who.int/mediacentre/news/releases/2014/amr-report/en/.
[3] E. A. Azzopardi, E. L. Ferguson, D. W. Thomas, *J. Antimicrob. Chemother.* **2013**, *68*, 257.
[4] H. Nikaido, J.-M. Pagès, *FEMS Microbiol. Rev.* **2012**, *36*, 340.
[5] T. Strateva, D. Yordanov, *J. Med. Microbiol.* **2009**, *58*, 1133.
[6] Z. Drulis-Kawa, J. Gubernator, A. Dorotkiewicz-Jach, W. Doroskiewicz, A. Kozubek, *Int. J. Pharm.* **2006**, *315*, 59.
[7] H. P. Schweizer, *Expert Opin. Drug Discovery* **2012**, *7*, 633.
[8] R. E. W. Hancok, *Clin. Infect. Dis.* **1998**, *27*, S93.
[9] A. D. Richards, A. Rodger, M. J. Hannon, A. Bolhuis, *Int. J. Antimicrob. Agents* **2009**, *33*, 469.
[10] N. S. Ng, P. Leverett, D. E. Hibbs, Q. Yang, J. C. Bulanadi, M. J. Wu, J. R. Aldrich-Wright, *Dalton Trans.* **2013**, *42*, 3196.
[11] M. A. Neelakantan, M. Esakkiammal, S. S. Mariappan, J. Dharmaraja, T. Jeyakumar, *Indian J. Pharm. Sci.* **2010**, *72*, 216.
[12] F. P. Dwyer, E. C. Gyarfas, W. P. Rogers, J. H. Koch, *Nature* **1952**, *170*, 190.
[13] F. P. Dwyer, I. K. Reid, A. Shulman, G. M. Laycock, S. Dixson, *Aust. J. Exp. Biol. Med. Sci.* **1969**, *47*, 203.
[14] A. Bolhuis, L. Hand, J. E. Marshall, A. D. Richards, A. Rodger, J. Aldrich-Wright, *Eur. J. Pharm. Sci.* **2011**, *42*, 313.
[15] C. Shobha Devi, D. A. Kumar, S. S. Singh, N. Gabra, N. Deepika, Y. P. Kumar, S. Satyanarayana, *Eur. J. Med. Chem.* **2013**, *64*, 410.
[16] F. Li, Y. Mulyana, M. Feteri, J. Warner, J. G. Collins, F. R. Keene, *Dalton Trans.* **2011**, *40*, 5032.
[17] M. Pandrala, F. Li, M. Feterl, Y. Mulyana, J. M. Warner, L. Wallace, F. R. Keene, J. G. Collins, *Dalton Trans.* **2013**, *42*, 4686.
[18] A. K. Gorle, M. Feterl, J. M. Warner, L. Wallace, F. R. Keene, J. G. Collins, *Dalton Trans.* **2014**, *43*, 16713.
[19] F. Li, M. Feterl, Y. Mulyana, J. M. Warner, J. G. Collins, F. R. Keene, *J. Antimicrob. Chemother.* **2012**, *67*, 2686.
[20] B. M. Zeglis, V. C. Pierre, J. K. Barton, *Chem. Commun.* **2007**, 4565.
[21] C. Metcalfe, J. A. Thomas, *Chem. Soc. Rev.* **2003**, *32*, 215.
[22] F. R. Keene, J. A. Smith, J. G. Collins, *Coord. Chem. Rev.* **2009**, *253*, 2021.
[23] M. R. Gill, J. A. Thomas, *Chem. Soc. Rev.* **2012**, *41*, 3179.
[24] A. J. Pryde, E. L. Shaw, E. Weeks, *J. Chem. Soc. Chem. Commun.* **1973**, 947.
[25] Although microscopy techniques that involve luminescence are conventionally referred to as "fluorescence microscopy", the luminescence is in fact phosphorescence in the case of the polypyridylruthenium(II) complexes because emission involves a transition from a triplet excited state to a singlet ground state, whereas fluorescence involves a transition between singlet excited and ground states.
[26] F. Li, E. J. Harry, A. L. Bottomley, M. D. Edstein, G. W. Birrell, C. E. Woodward, F. R. Keene, J. G. Collins, *Chem. Sci.* **2014**, *5*, 685.
[27] A. Srishailam, N. M. Gabra, Y. P. Kumar, K. L. Reddy, C. S. Devi, D. A. Kumar, S. S. Singh, S. Satyanarayana, *J. Photochem. Photobiol. B* **2014**, *141*, 47.
[28] H. Nikaido, *Science* **1994**, *264*, 382.
[29] S. Tamber, E. Maier, R. Benz, R. E. W. Hancock, *J. Bacteriol.* **2007**, *189*, 929.

[30] X. Li, A. K. Gorle, T. D. Ainsworth, K. Heimann, C. E. Woodward, J. G. Collins, F. R. Keene, *Dalton Trans.* **2015**, *44*, 3594.
[31] Y. Mulyana, D. K. Weber, P. D. Buck, C. A. Motti, J. G. Collins, F. R. Keene, *Dalton Trans.* **2011**, *40*, 1510.
[32] I. P. Evans, A. Spencer, G. Wilkinson, *J. Chem. Soc. Dalton Trans.* **1973**, 204.
[33] H. A. Hudali, J. V. Kingston; H. A. Tayim, *Inorg. Chem.* **1979**, *18*, 1391; H. A. Tayim, *Inorg. Chem.* **1979**, *18*, 1391.
[34] Clinical and Laboratory Standards Institute. Performance Standards for Antimicrobial Susceptibility Testing: Nineteenth Informational Supplement M100-S19. CLSI, Wayne, PA, USA, **2009**.

Received: January 29, 2015
Published online on ■■ ■■, 0000

FULL PAPER

New activity: The inert mononuclear ruthenium(II) complex *cis*-α-[Ru(phen)(bb_{12})]$^{2+}$ ion (see picture; phen = 1,10-phenanthroline, bb = bis[4(4′-methyl-2,2′-bipyridyl)]-1,*n*-alkane) readily accumulates in *Pseudomonas aeruginosa* and showed good activity against it. This Gram-negative bacterium is of particular worldwide concern because it is naturally resistant to many antimicrobial agents due to the low permeability of its outer membrane.

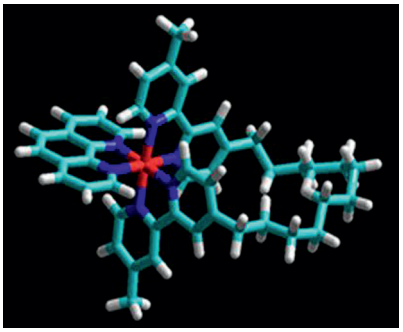

Metal-Based Antimicrobial Drugs

A. K. Gorle, M. Feterl, J. M. Warner, S. Primrose, C. C. Constantinoiu, F. R. Keene, J. G. Collins**

■■ – ■■

Mononuclear Polypyridylruthenium(II) Complexes with High Membrane Permeability in Gram-Negative Bacteria—in particular *Pseudomonas aeruginosa*